Operator Relaxation and the Optimal Depth of Classical Shadows

Matteo Ippoliti, Yaodong Li, Tibor Rakovszky, and Vedika Khemani

Phys. Rev. Lett. **130**, 230403 — Published 9 June 2023

DOI: 10.1103/PhysRevLett.130.230403

Operator relaxation and the optimal depth of classical shadows

Matteo Ippoliti, Yaodong Li, Tibor Rakovszky, and Vedika Khemani
Department of Physics, Stanford University, Stanford, CA 94305, USA

Classical shadows are a powerful method for learning many properties of quantum states in a sample-efficient manner, by making use of randomized measurements. Here we study the sample complexity of learning the expectation value of Pauli operators via "shallow shadows", a recently-proposed version of classical shadows in which the randomization step is effected by a local unitary circuit of variable depth t. We show that the shadow norm (the quantity controlling the sample complexity) is expressed in terms of properties of the Heisenberg time evolution of operators under the randomizing ("twirling") circuit—namely the evolution of the *weight distribution* characterizing the number of sites on which an operator acts nontrivially. For spatially-contiguous Pauli operators of weight k, this entails a competition between two processes: *operator spreading* (whereby the support of an operator grows over time, increasing its weight) and *operator relaxation* (whereby the bulk of the operator develops an equilibrium density of identity operators, decreasing its weight). From this simple picture we derive (i) an upper bound on the shadow norm which, for depth $t \sim \log(k)$, guarantees an exponential gain in sample complexity over the $t = 0$ protocol in any spatial dimension, and (ii) quantitative results in one dimension within a mean-field approximation, including a universal subleading correction to the optimal depth, found to be in excellent agreement with infinite matrix product state numerical simulations. Our work connects fundamental ideas in quantum many-body dynamics to applications in quantum information science, and paves the way to highly-optimized protocols for learning different properties of quantum states.

Introduction. The development of controllable quantum simulators has enabled the creation of complex and highly entangled quantum states in laboratory settings, leading to exciting new developments in quantum information science and many-body physics [1–8]. These advances raise the issue of how to efficiently characterize such quantum states. Full quantum state tomography requires exponentially many measurements in the size of the system [9], motivating the need for more scalable and efficient state-learning protocols. Recent progress in this direction has come from the development of *classical shadows* [10–22], a method to extract many physical properties of states with a dramatically smaller number of measurements. In this work, we shed light on the inner workings of classical shadows by making connections to foundational ideas in quantum dynamics on the spreading and equilibration of operators.

Classical shadows use *randomized measurements* [23–25] to form a compact representation of a many-body quantum state, Fig. 1(a). The state ρ is first transformed by a random unitary operation U (chosen from a suitable "twirling ensemble"), then projectively measured, yielding a computational basis state $|b\rangle$. The measured basis state is then rotated backwards (on a classical computer), giving a "snapshot" $\hat{\sigma}_{U,b} = U^\dagger |b\rangle\langle b| U$. The average of these snapshots (over twirling unitaries and measurement outcomes) is related to the true state ρ by a quantum channel, $\mathbb{E}_{U,b}[\hat{\sigma}_{U,b}] = \mathcal{M}(\rho)$. If the measurements are *tomographically complete* [11], the channel $\mathcal{M}$ can be inverted (again on a classical computer) to produce "inverted snapshots" $\hat{\rho}_{U,b} = \mathcal{M}^{-1}(\hat{\sigma}_{U,b})$. These form a compact, approximate description of the quantum state ρ—its *classical shadow* [11]. From this description one can extract many properties of the state, which remarkably do not have to be specified in advance—the general philosophy of the method is to *"measure first, ask questions later"* [25].

The usefulness of classical shadows depends on their *sample complexity*, i.e., the number of experimental samples needed in order to estimate a certain property of ρ within a given error. To learn an expectation value $\mathrm{Tr}(\rho O)$, one builds estimators $\hat{o}_{U,b} = \mathrm{Tr}(\hat{\rho}_{U,b} O)$ that yield the desired value in expectation ($\mathbb{E}_{U,b}[\hat{o}_{U,b}] = \mathrm{Tr}(\rho O)$). The sample complexity is determined by the variance of $\hat{o}$, captured by the *shadow norm* $\|O\|_{\mathrm{sh}}$, itself a function of the twirling ensemble. The freedom in choosing the twirling ensemble can thus be leveraged to optimize the learnability of certain properties of a quantum state. For instance, "local twirling" (where $U = \bigotimes_i u_i$ is a product of single-qubit random unitaries) gives $\|O\|^2_{\mathrm{sh}} = 3^k$ for Pauli operators, where k is the number of qubits on which O acts nontrivially; this is best suited to learning the value of few-body operators. On the opposite end, "global twirling" (where U is a random Clifford unitary on the whole Hilbert space) gives $\|O\|^2_{\mathrm{sh}} = \mathrm{Tr}(O^\dagger O)$, which favors learning e.g. the fidelity with a pure many-body state $O = |\psi\rangle\langle\psi|$, but performs poorly on Pauli operators ($\|O\|^2_{\mathrm{sh}} = 2^N$) irrespective of locality [11].

Intermediate schemes, dubbed *shallow shadows*, have been recently proposed [26–28] and use twirling ensembles made of shallow quantum circuits, whose depth t can be tuned to interpolate between the local and global twirling limits. The finite depth t makes these easier to implement on quantum hardware, and enables efficient classical computation of $\hat{\sigma}$ and $\hat{\rho}$ via tensor-network methods [26, 27]. Surprisingly, these schemes were numerically observed to perform better than local twirling for estimating the expectation value of contiguous, multi-site Pauli operators (interesting examples of such operators include string order parameters for characterizing

topological phases [29, 30] and check operators of a quantum code [31]). The optimal depth $t^\star(k)$ for a Pauli operator acting on k contiguous sites was observed numerically to scale as polylog(k) in one dimension [26], with a significant gain in sample complexity over the local twlirling protocol. The physical mechanism behind this behavior has remained elusive thus far.

Here we analyze this problem analytically and find a mapping of the shadow norm to the dynamics of *Hamming weight* (the number of sites on which a Pauli operator acts nontrivially, henceforth just 'weight') under the twirling evolution. This mapping reveals that the optimal depth for the estimation of contiguous Pauli operators is determined by the competition of two processes under chaotic unitary dynamics, sketched in Fig. 1(b): *operator spreading* [32–37] and *operator relaxation*, to be defined below. Based on this picture, we prove that at depth $t^\star(k) \sim \log(k)$, shallow shadows realize an exponential-in-k gain in sample complexity over local twirling in any finite spatial dimension. We further develop an analytical mean-field approximation for the shadow norm in one dimension, indicating that at depth $t^\star(k)$ the sample complexity nearly saturates a lower bound ($\sim 2^k$, up to poly(k) corrections), as sketched in Fig. 1(c); the prediction shows excellent agreement with numerics on large Pauli operators (up to $k = 1000$) in infinite 1D systems.

Our results shed light on the inner workings of the classical shadows protocol and how it relates to fundamental aspects of quantum dynamics. At the same time, they give a practical, operational meaning to ideas about operator dynamics, and promise applications towards highly optimized classical shadows protocols for near-term quantum devices.

Shadow norm and operator weight. We begin by deriving a relationship between the shadow norm and operator dynamics valid if the twirling ensemble is *locally scrambled* [38, 39], i.e., such that measure $\mathrm{d}U$ over the ensemble is invariant under $U \mapsto VU$ and $U \mapsto UV$ for all product Clifford unitaries [40] $V = \bigotimes_i v_i$, $v_i \in \mathsf{Cliff}(q)$ (this holds for local and global twirling, as well as for shallow shadows [26–28]).

We will consider a system of q-state qudits arranged on a d-dimensional lattice consisting of N qudits. For qudits with $q > 2$, we use "generalized Pauli operators" defined by products of clock and shift unitary operators [41]. The measurement channel reads

$$\mathcal{M}(\rho) = \sum_b \int \mathrm{d}U \overbrace{\langle b|\, U\rho U^\dagger \,|b\rangle}^{\mathrm{Prob}(b|\rho,U)} \overbrace{U^\dagger\,|b\rangle\langle b|\, U}^{\text{snapshot } \hat{\sigma}_{U,b}}, \qquad (1)$$

where b ranges over all $D = q^N$ computational basis states.

All Pauli operators are eigenmodes of the channel [20, 26, 27], and the eigenvalue depends solely on the twirling ensemble and on the support A of the Pauli operator: $\mathcal{M}[O_A] = \lambda_A O_A$, where O_A denotes a Pauli operator

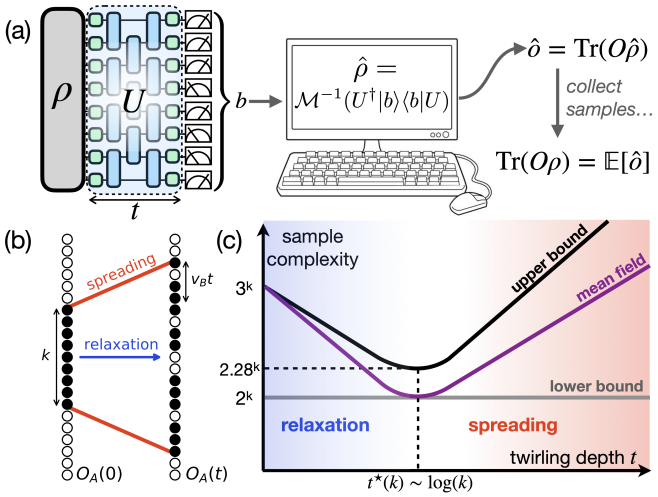

FIG. 1. (a) Schematic of classical shadows via shallow circuits: a state ρ is randomized by a "twirling" circuit U of depth t, then measured; data is classically processed to estimate Pauli expectation values. (b) Operator spreading and relaxation under chaotic dynamics. ○/● denote identity and traceless Pauli matrices, respectively. (c) Summary of main results of this work. The competition between operator spreading and relaxation determines the optimal sample complexity of learning Pauli expectation values.

supported in region A. The eigenvalues can be expressed as [42]

$$\lambda_A = \sum_{w=1}^{N} \pi_{A,t}(w)(q+1)^{-w}, \qquad (2)$$

where $\pi_{A,t}(w)$ is the averaged *weight distribution* [43] of the twirled operator $O_A(t) \equiv UO_AU^\dagger$:

$$\pi_{A,t}(w) = \sum_{P:\ |P|=w} \mathbb{E}_U \left|D^{-1}\mathrm{Tr}(PO_A(t))\right|^2. \qquad (3)$$

The sum runs over Pauli operators P, and $|P|$ is the weight of P.

With this result, we can exactly compute the shadow norm: $\|O_A\|^2_{\mathrm{sh}} = \mathrm{Tr}(O_A^\dagger \mathcal{M}^{-1}[O_A])/D = \lambda_A^{-1}$ [26, 27, 42]. Combined with Eq. (2), this yields an exact relationship between the shadow norm and the weight distribution of a twirled operator,

$$\|O_A\|^2_{\mathrm{sh}} = \left[\overline{(q+1)^{-w}}\right]^{-1} \qquad (4)$$

where the overline denotes averaging over w according to $\pi_{A,t}(w)$. Eq. (4) constitutes one of the main results of our work.

Eq. (4) reproduces the well-known results for local and global twirling of qubits (3^k and 2^N respectively [11]) in the $t = 0$ and $t \to \infty$ limits [42]. However, our result allows us to understand the behavior of the shadow norm away from these well-know limits, by leveraging the connection to the dynamics of operator weight under chaotic

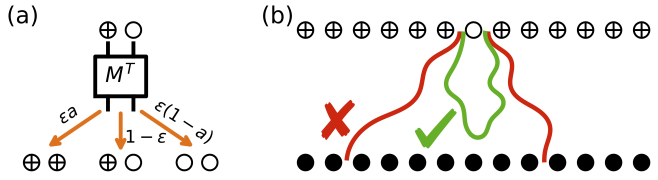

FIG. 2. (a) Update rules for a domain wall between $\oplus$ and $\bigcirc$ states. (b) Random-walk calculation for the average density of holes $\overline{h_i}(t)$: if the two walkers fail to annihilate within t steps, the diagram vanishes.

evolution (i.e. the twirling ensemble U) as a function of time (i.e. the variable depth t).

Relaxation of operator weight. We focus on Pauli operators whose support A is a spatially-contiguous region (though our results also have implications for more general, non-contiguous Pauli operators [42]). We consider twirling ensembles of *diluted* random brickwork circuits, i.e. circuits where each gate is Haar-random [44] with probability ϵ and is the identity otherwise. These include conventional random circuits ($\epsilon = 1$), but allow us to slow down the twirling dynamics and discretize time more finely. To study the dynamics of operator weight during twirling, we introduce "occupation" variables n_i ($n_i = 0$ if a Pauli operator is the identity at site i, $n_i = 1$ otherwise). Before twirling, we have a *fully-packed* Pauli operator in region A: $n_i = 1$ iff $i \in A$. As the twirling depth t increases, two things happen: (i) *Operator spreading*—the boundary of the operator moves outwards, so that $\overline{n_i}(t) > 0$ also on sites $i \notin A$ that were initially empty, leading to an *increase* in weight; and (ii) *Operator relaxation*—the bulk of the operator relaxes from its fully-packed initial state ($n_i = 1\ \forall\ i \in A$) towards an equilibrium density $\overline{n_i}(t) \to 1 - q^{-2}$ (when all q^2 Pauli operators are equally likely), leading to a *decrease* in weight.

As the latter is a bulk effect, it always dominates (at early times) for a sufficiently large region A. Thus the shadow norm must initially decrease from its $t = 0$ value (local twirling), before eventually becoming dominated by operator spreading and increasing again towards its $t \to \infty$ value (global twirling), implying a minimum at some finite optimal depth $t^\star$.

To characterize the relaxation process, we focus on an infinite, fully-packed Pauli operator, and consider the average occupation of a site $\overline{n_i}(t)$ as a function of twirling depth t. For the twirling ensembles under consideration this problem can be addressed analytically in one spatial dimension. We leverage the fact that the vector of occupation probabilities $p_{\mathbf{n}}$ ($\mathbf{n} \in \{0,1\}^N$ labels occupation configurations) evolves under the circuit-averaged dynamics via a Markov process, $p'_{\mathbf{n}} = \sum_{\mathbf{m}} \mathbb{M}_{\mathbf{n},\mathbf{m}} p_{\mathbf{m}}$ with $\mathbb{M}$ a stochastic matrix ($\sum_{\mathbf{m}} \mathbb{M}_{\mathbf{m},\mathbf{n}} = 1\ \forall \mathbf{n}$), to solve for the local occupation number analytically [34, 36]. We focus on the "density of holes" $\overline{h_i}$ ($h_i \equiv 1 - n_i$) and introduce vectors in the binary space of (identity, traceless Pauli): $|\bigcirc) = (1,0)^T$, $|\bullet) = (0,1)^T$, and $|\oplus) = (1,1)^T$. The fully-packed initial state $p^{\text{init}}_{\mathbf{n}} = \prod_i \delta_{n_i,1}$ evolves under the averaged circuit into a final state $p^{\text{final}}_{\mathbf{n}}$, and we have $\overline{h_i} = \sum_{\mathbf{n}} p^{\text{final}}_{\mathbf{n}} \delta_{n_i,0}$, corresponding to a matrix element $(\cdots\oplus\oplus\bigcirc\oplus\oplus\cdots|\mathbb{M}_t|\cdots\bullet\bullet\bullet\cdots)$ where $\mathbb{M}_t$ is the transition matrix for the averaged depth-t twirling circuit.

It is advantageous to consider the *backward* evolution $\mathbb{M}_t^T$ acting on the state $|\cdots\oplus\oplus\oplus\bigcirc\oplus\oplus\oplus\cdots)$: we have $M^T|\oplus\bigcirc) = \epsilon a|\oplus\oplus) + (1-\epsilon)|\oplus\bigcirc) + \epsilon(1-a)|\bigcirc\bigcirc)$ (Fig. 2(a)), where M is the transition matrix for a single two-qudit gate, $a = 1/(q^2+1)$, and ϵ is the dilution parameter (see [42]). Moreover we have $M^T|\bigcirc\bigcirc) = |\bigcirc\bigcirc)$ (unitary invariance of the identity operator) and $M^T|\oplus\oplus) = |\oplus\oplus)$ (conservation of total probability under the Markov process [45]). Thus the structure of a domain of $\bigcirc$ in a background of $\oplus$ is preserved under $\mathbb{M}_t^T$, and domain walls undergo a random walk with a bias that tends to expand the $\bigcirc$ domain. When the domain walls are adjacent, they may annihilate, leading to an all-$\oplus$ state which is invariant under M^T and yields a contribution $(\oplus|\bullet)^N = 1$; if the domain of $\bigcirc$ survives all the way to $t = 0$, the result vanishes as it involves at least one overlap $(\bigcirc|\bullet) = 0$ (Fig. 2(b)).

In all, the average density of holes $\overline{h_i}(t)$ equals the probability that the two random walkers annihilate in t steps or less; conversely, $\overline{n_i}(t)$ equals their *survival probability*, which can be computed analytically: at large t,

$$\overline{n_i}(t) = 1 - q^{-2} + ct^{-3/2}e^{-\gamma t} + \dots \tag{5}$$

for any site i in the bulk of the operator, with $c > 0$ a constant and $\dots$ denoting subleading corrections in t [42]. The relaxation rate γ is related to the circuit's *entanglement velocity* v_E (which sets the decay of half-system purity as $\sim q^{-v_E t}$) [46] via $\gamma = 2\ln(q)v_E$, see [42]; the $t^{-3/2}$ is a universal correction related to the first return of a random walker in one dimension [47]. We conjecture that the convergence to equilibrium is exponential in any finite spatial dimension, and numerically verify it in two dimensions [42].

Scaling of the optimal depth. With these key results in hand, we return to the question of the optimal depth. From Eq. (4) and Jensen's inequality, we have $\|O_A\|^2_{\text{sh}} \le (q+1)^{\overline{w}}$; in one dimension, the average weight obeys $\overline{w}(t) = \sum_i \overline{n_i}(t) \simeq \overline{\ell}(t)\overline{n_{\text{bulk}}}(t)$, with $\overline{\ell}(t) = k + 2v_B t$ the average spatial length of the twirled operator, which spreads with butterfly velocity v_B [34, 36, 48], and $\overline{n_{\text{bulk}}}(t)$ the bulk density of traceless Paulis, Eq. (5) (the structure of the operator's fronts can be neglected at large k). The bound is minimized at depth

$$t^\star(k) = \gamma^{-1}\left(\ln(k) - \frac{3}{2}\ln\ln(k) + o(\ln\ln(k))\right) \tag{6}$$

(see [42]). At $t = t^\star(k)$, the shadow norm is bounded above by $(q+1)^{(1-q^{-2})k} \times \text{poly}(k)$, *exponentially smaller* than the $t = 0$ (local twirling) value of $(q+1)^k$; e.g., for qubits ($q = 2$) the scaling is $3^{\frac{3}{4}k} \simeq 2.28^k$ vs 3^k. The scaling $\log(k)$ (as opposed to more general polylog(k) [26])

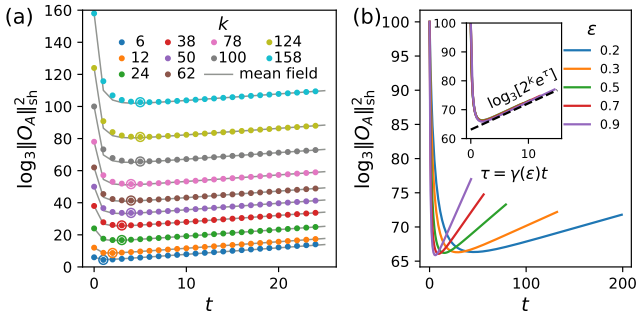

FIG. 3. (a) Shadow norm of a weight-k Pauli string O_A in an infinite 1D system of qubits ($q = 2$), under twirlig by depth-t brickwork circuits of Haar-random gates (no gate dilution, $\epsilon = 1$). Data from iMPS simulations with bond dimension $\chi = 2048$. Circled dots indicate the optimal depth. (b) Same quantity for fixed $k = 100$ and variable gate dilution ϵ. Inset: same data as a function of "effective depth" $\tau = \gamma(\epsilon)t$, compared to $q^k e^{\gamma t}$ (dashed line).

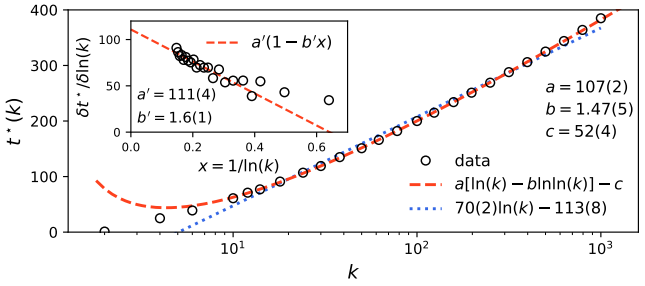

FIG. 4. Optimal depth $t^\star(k)$ as a function of Pauli operator weight k, obtained from iMPS data as in Fig. 3, for k up to 1000. The gate dilution is $\epsilon = 0.05$ and bond dimension is $\chi = 2048$. Best fits to $t^\star(k) = a'' \ln(k) - c''$ (dotted line) and $t^\star(k) = a[\ln(k) - b \ln\ln(k)] - c$ (dashed line) are shown. The doubly-logarithmic correction is found to be $b = 1.47(5)$, consistent with the predicted 3/2 in Eq. (6). Inset: discrete derivatives $\delta t^\star(k)/\delta \ln(k)$, plotted vs $1/\ln(k)$, indicate a doubly-logarithmic correction $b = 1.6(1)$, also consistent with 3/2.

is especially important as it ensures an MPO representation for $\mathcal{M}^{-1}$ with poly(k) bond dimension, key to the classical computational cost of the method [26, 27].

We conjecture that $t = t^\star(k)$ minimizes not just the upper bound $(q+1)^{\overline{w}}$, but the shadow norm itself, and that the achievable scaling of the latter is poly(k)$\times q^k$—nearly saturating the q^k lower bound obtained by full relaxation with no spreading. This is supported by an analytical calculation within a mean-field approximation, where we neglect correlations between occupations n_i, n_j at different sites, see [42]. We find that $\|O_A\|_{\rm sh}$ is dominated by Pauli operators of size $k + 2v_B^{\rm sp} t$, with a renormalized "saddle-point butterfly velocity" $v_B^{\rm sp}$ smaller than the original v_B, and equal to the entanglement velocity $v_E = \gamma/\ln(q^2)$. This predicts the late-time behavior $\|O_A\|^2_{\rm sh} \sim q^{k+2v_B^{\rm sp}t} = q^k e^{\gamma t}$. Minimizing the mean-field shadow norm over t yields the same $t^\star(k)$ as in Eq. (6), and thus the optimal shadow norm $\sim kq^k$.

It follows also that shallow shadows can be advantageous over local twirling not just for operators with contiguous support, but also for various types of non-contiguous operators, notably including typical random Pauli strings on a finite segment [42].

Numerical simulations. To check the validity of the above results, we perform numerical simulations of the averaged twirling dynamics with infinite matrix product states (iMPS) [49] (see [42]). Fig. 3(a) shows the shadow norm for contiguous operators in a 1D chain of qubits ($q = 2$), as a function of depth t. Three regimes are clearly visible: the $t = 0$ (local-twirling) value of 3^k, a minimum at $t \sim \log(k)$, and finally exponential growth due to continued operator spreading after relaxation. In un-diluted circuits ($\epsilon = 1$) the optimal depth $t^\star(k)$ takes very small integer values, severely limiting the resolution on its scaling [26]. This issue is greatly alleviated by gate dilution: the shadow norm approximately behaves as a smooth function of an "effective depth" $\tau = \gamma(\epsilon)t$ (Fig. 3(b)), where γ is the Pauli density relaxation rate in Eq. (5)—smaller ϵ yields a finer sampling of τ. To finely resolve the scaling of $t^\star(k)$, we set $\epsilon = 0.05$ obtaining the results in Fig. 4. The data show remarkable agreement with Eq. (6), including the subleading correction $\sim \ln\ln(k)$. The value of 3/2 for the ratio of coefficients is universal (determined by the probability of first return of a random walk via Eq. (5)), which constitutes a non-trivial check of our analytical results.

Higher dimensions. While several details of the above discussion are special to one dimension, the general picture applies to systems in any finite spatial dimension. The leading-order result ($t^\star(k) \sim \ln k$) depends only on the balancing of operator spreading and relaxation for operators whose boundary is much smaller than the bulk. In systems with all-to-all connectivity or on expander graphs, where a subsystem's bulk and boundary generally have comparable sizes, the optimal twirling depth is expected to be zero, i.e., local twirling performs best. We test this expectation on a "Brownian circuit" model whose operator dynamics are described by simple, closed equations, and are amenable to exact treatment; we find the optimal depth is $t = 0$ unless the operator is supported on a sufficiently large fraction of the system ($k \gtrsim N/2$), see [42].

Discussion. We have studied how classical shadows based on shallow quantum circuits can be used to learn expectation values of Pauli operators. We have connected the sample complexity of classical shadows to the dynamics of operator weight, identifying two competing dynamical processes (operator spreading and relaxation) whose balance determines the optimal depth $t^\star$ of the twirling circuits. This picture elegantly explains previous numerical observations on one-dimensional systems [26, 27], and extends the result to systems in any finite dimension. Further, it shows that the optimal depth scales as

$t^\star = O(\ln k)$ with the weight k of the learned operator, as opposed to a more general $t^\star = \text{polylog}(k)$ scaling [26], ensuring a poly(k) classical computational cost for the optimal protocol.

Our work opens up several directions for future research. It would be interesting to generalize our results to different settings for classical shadows, beyond shallow brickwork circuits on qudits. The recent proposals for classical shadows in analog simulators [50, 51] or on fermionic [17, 18] and bosonic [52] systems are interesting possible directions. The validity of our results in higher dimension also suggests interesting applications to e.g. topological or fracton codes and phases [53–58]. Further, it would be interesting to extend our analysis to measures of entanglement [23, 24], and to make contact with NISQ experiments [15, 59] by understanding the impact of noise on our results [13, 60].

Finally, the concept of operator relaxation may be of independent interest from the point of view of quantum dynamics. While operator spreading is central to the study of quantum chaos [32–37], operator relaxation and similar diagnostics of local equilibration in operator space [35, 37, 61] are comparatively under-explored, and may prove similarly useful in understanding signatures of quantum-chaotic behavior [62].

ACKNOWLEDGMENTS

Acknowledgments. We thank Bryan Clark, Wen Wei Ho and Hsin-Yuan Huang for discussions on classical shadows. M.I. and Y.L. are supported in part by the Gordon and Betty Moore Foundation's EPiQS Initiative through Grant GBMF8686. T.R and Y.L. are supported in part by the Stanford Q-FARM Bloch Postdoctoral Fellowship in Quantum Science and Engineering. V.K. acknowledges support from the US Department of Energy, Office of Science, Basic Energy Sciences, under Early Career Award Nos. DE-SC0021111, the Alfred P. Sloan Foundation through a Sloan Research Fellowship, and the Packard Foundation through a Packard Fellowship in Science and Engineering. Numerical simulations were performed on Stanford Research Computing Center's Sherlock cluster. We acknowledge the hospitality of the Kavli Institute for Theoretical Physics at the University of California, Santa Barbara (supported by NSF Grant PHY-1748958).

[1] Frank Arute, Kunal Arya, Ryan Babbush, Dave Bacon, Joseph C. Bardin, Rami Barends, Rupak Biswas, Sergio Boixo, *et al.*, "Quantum supremacy using a programmable superconducting processor," Nature **574**, 505–510 (2019).

[2] Ehud Altman, Kenneth R. Brown, Giuseppe Carleo, Lincoln D. Carr, Eugene Demler, Cheng Chin, Brian DeMarco, Sophia E. Economou, *et al.*, "Quantum Simulators: Architectures and Opportunities," PRX Quantum **2**, 017003 (2021).

[3] Xiao Mi, Pedram Roushan, Chris Quintana, Salvatore Mandra, Jeffrey Marshall, Charles Neill, Frank Arute, Kunal Arya, *et al.*, "Information scrambling in quantum circuits," Science **374**, 1479–1483 (2021).

[4] Yulin Wu, Wan-Su Bao, Sirui Cao, Fusheng Chen, Ming-Cheng Chen, Xiawei Chen, Tung-Hsun Chung, Hui Deng, *et al.*, "Strong Quantum Computational Advantage Using a Superconducting Quantum Processor," Physical Review Letters **127**, 180501 (2021).

[5] Laird Egan, Dripto M. Debroy, Crystal Noel, Andrew Risinger, Daiwei Zhu, Debopriyo Biswas, Michael Newman, Muyuan Li, *et al.*, "Fault-tolerant control of an error-corrected qubit," Nature **598**, 281–286 (2021).

[6] Rajeev Acharya, Igor Aleiner, Richard Allen, Trond I. Andersen, Markus Ansmann, Frank Arute, Kunal Arya, Abraham Asfaw, *et al.*, "Suppressing quantum errors by scaling a surface code logical qubit," Nature **614**, 676–681 (2023).

[7] Sepehr Ebadi, Tout T. Wang, Harry Levine, Alexander Keesling, Giulia Semeghini, Ahmed Omran, Dolev Bluvstein, Rhine Samajdar, *et al.*, "Quantum phases of matter on a 256-atom programmable quantum simulator," Nature **595**, 227–232 (2021).

[8] G. Semeghini, H. Levine, A. Keesling, S. Ebadi, T. T. Wang, D. Bluvstein, R. Verresen, H. Pichler, *et al.*, "Probing topological spin liquids on a programmable quantum simulator," Science **374**, 1242–1247 (2021).

[9] Jeongwan Haah, Aram W. Harrow, Zhengfeng Ji, Xiaodi Wu, and Nengkun Yu, "Sample-Optimal Tomography of Quantum States," IEEE Transactions on Information Theory **63**, 5628–5641 (2017).

[10] Scott Aaronson, "Shadow Tomography of Quantum States," (2018), 10.48550/arXiv.1711.01053.

[11] Hsin-Yuan Huang, Richard Kueng, and John Preskill, "Predicting many properties of a quantum system from very few measurements," Nature Physics **16**, 1050–1057 (2020).

[12] Marco Paini and Amir Kalev, "An approximate description of quantum states," (2019), 10.48550/arXiv.1910.10543.

[13] Senrui Chen, Wenjun Yu, Pei Zeng, and Steven T. Flammia, "Robust Shadow Estimation," PRX Quantum **2**, 030348 (2021).

[14] Atithi Acharya, Siddhartha Saha, and Anirvan M. Sengupta, "Shadow tomography based on informationally complete positive operator-valued measure," Physical Review A **104**, 052418 (2021).

[15] G.I. Struchalin, Ya. A. Zagorovskii, E.V. Kovlakov, S.S. Straupe, and S.P. Kulik, "Experimental Estimation of Quantum State Properties from Classical Shadows," PRX Quantum **2**, 010307 (2021).

[16] Ryan Levy, Di Luo, and Bryan K. Clark, "Classical Shadows for Quantum Process Tomography on Near-term Quantum Computers," (2021), 10.48550/arXiv.2110.02965.

[17] Andrew Zhao, Nicholas C. Rubin, and Akimasa Miyake,

"Fermionic Partial Tomography via Classical Shadows," Physical Review Letters **127**, 110504 (2021).
[18] Kianna Wan, William J. Huggins, Joonho Lee, and Ryan Babbush, "Matchgate Shadows for Fermionic Quantum Simulation," (2022), 10.48550/arXiv.2207.13723.
[19] Hsin-Yuan Huang, Richard Kueng, Giacomo Torlai, Victor V. Albert, and John Preskill, "Provably efficient machine learning for quantum many-body problems," Science **377**, eabk3333 (2022).
[20] Kaifeng Bu, Dax Enshan Koh, Roy J. Garcia, and Arthur Jaffe, "Classical shadows with Pauli-invariant unitary ensembles," (2022), 10.48550/arXiv.2202.03272.
[21] Jonathan Kunjummen, Minh C. Tran, Daniel Carney, and Jacob M. Taylor, "Shadow process tomography of quantum channels," Physical Review A **107**, 042403 (2023).
[22] Saumya Shivam, C. W. von Keyserlingk, and S. L. Sondhi, "On Classical and Hybrid Shadows of Quantum States," (2022), 10.48550/arXiv.2206.06616.
[23] A. Elben, B. Vermersch, C. F. Roos, and P. Zoller, "Statistical correlations between locally randomized measurements: A toolbox for probing entanglement in many-body quantum states," Phys. Rev. A **99**, 052323 (2019).
[24] Tiff Brydges, Andreas Elben, Petar Jurcevic, Benoit Vermersch, Christine Maier, Ben P. Lanyon, Peter Zoller, Rainer Blatt, *et al.*, "Probing Renyi entanglement entropy via randomized measurements," Science **364**, 260–263 (2019).
[25] Andreas Elben, Steven T. Flammia, Hsin-Yuan Huang, Richard Kueng, John Preskill, Benoit Vermersch, and Peter Zoller, "The randomized measurement toolbox," Nature Reviews Physics **5**, 9–24 (2023).
[26] Ahmed A. Akhtar, Hong-Ye Hu, and Yi-Zhuang You, "Scalable and Flexible Classical Shadow Tomography with Tensor Networks," (2022), 10.48550/arXiv.2209.02093.
[27] Christian Bertoni, Jonas Haferkamp, Marcel Hinsche, Marios Ioannou, Jens Eisert, and Hakop Pashayan, "Shallow shadows: Expectation estimation using low-depth random Clifford circuits," (2022), 10.48550/arXiv.2209.12924.
[28] Mirko Arienzo, Markus Heinrich, Ingo Roth, and Martin Kliesch, "Closed-form analytic expressions for shadow estimation with brickwork circuits," (2022), 10.48550/arXiv.2211.09835.
[29] Tom Kennedy and Hal Tasaki, "Hidden $\mathbb{Z}_2 \times \mathbb{Z}_2$ symmetry breaking in Haldane-gap antiferromagnets," Physical Review B **45**, 304–307 (1992).
[30] Jutho Haegeman, David Perez-Garcia, Ignacio Cirac, and Norbert Schuch, "Order Parameter for Symmetry-Protected Phases in One Dimension," Physical Review Letters **109**, 050402 (2012).
[31] Daniel Gottesman, "Stabilizer Codes and Quantum Error Correction," (1997), 10.48550/arXiv.quant-ph/9705052.
[32] Juan Maldacena, Stephen H. Shenker, and Douglas Stanford, "A bound on chaos," Journal of High Energy Physics **2016**, 106 (2016).
[33] Brian Swingle, Gregory Bentsen, Monika Schleier-Smith, and Patrick Hayden, "Measuring the scrambling of quantum information," Physical Review A **94**, 040302 (2016).
[34] Adam Nahum, Sagar Vijay, and Jeongwan Haah, "Operator Spreading in Random Unitary Circuits," Physical Review X **8**, 021014 (2018).
[35] Vedika Khemani, Ashvin Vishwanath, and David A. Huse, "Operator Spreading and the Emergence of Dissipative Hydrodynamics under Unitary Evolution with Conservation Laws," Phys. Rev. X **8**, 031057 (2018).
[36] C. W. von Keyserlingk, Tibor Rakovszky, Frank Pollmann, and S. L. Sondhi, "Operator Hydrodynamics, OTOCs, and Entanglement Growth in Systems without Conservation Laws," Physical Review X **8**, 021013 (2018).
[37] Tibor Rakovszky, Frank Pollmann, and C. W. von Keyserlingk, "Diffusive Hydrodynamics of Out-of-Time-Ordered Correlators with Charge Conservation," Phys. Rev. X **8**, 031058 (2018).
[38] Wei-Ting Kuo, A. A. Akhtar, Daniel P. Arovas, and Yi-Zhuang You, "Markovian Entanglement Dynamics under Locally Scrambled Quantum Evolution," Physical Review B **101**, 224202 (2020).
[39] Hong-Ye Hu, Soonwon Choi, and Yi-Zhuang You, "Classical Shadow Tomography with Locally Scrambled Quantum Dynamics," (2021), 10.48550/arXiv.2107.04817.
[40] Daniel Gottesman, "The Heisenberg Representation of Quantum Computers," (1998), 10.48550/arXiv.quant-ph/9807006.
[41] Vlad Gheorghiu, "Standard form of qudit stabilizer groups," Physics Letters A **378**, 505–509 (2014).
[42] See Supplementary Material for the derivation of Eq. (4) and Eq. (6), results on Brownian circuits, computation of velocity scales, estimation of non-contiguous operators, and additional details on the random walk mapping, mean-field approximation and numerical methods. The Supplementary Material includes Refs. [63–65].
[43] Xiao-Liang Qi, Emily J. Davis, Avikar Periwal, and Monika Schleier-Smith, "Measuring operator size growth in quantum quench experiments," (2019), 10.48550/arXiv.1906.00524.
[44] The same results would be obtained with any unitary 2-design (e.g. random Clifford gates).
[45] Note $(\oplus\oplus|p)$ yields the sum of the two-site probability distribution p_{n_1,n_2}; conservation of total probability, i.e. $(\oplus\oplus|M|p) = (\oplus\oplus|p)\ \forall p$, imposes $(\oplus\oplus|M = (\oplus\oplus|$.
[46] Adam Nahum, Jonathan Ruhman, Sagar Vijay, and Jeongwan Haah, "Quantum Entanglement Growth under Random Unitary Dynamics," Physical Review X **7**, 031016 (2017).
[47] Michael E. Fisher, "Walks, walls, wetting, and melting," Journal of Statistical Physics **34**, 667–729 (1984).
[48] Pavan Hosur, Xiao-Liang Qi, Daniel A. Roberts, and Beni Yoshida, "Chaos in quantum channels," Journal of High Energy Physics **2016**, 4 (2016).
[49] Ulrich Schollwock, "The density-matrix renormalization group in the age of matrix product states," Annals of Physics January 2011 Special Issue, **326**, 96–192 (2011).
[50] Minh C. Tran, Daniel K. Mark, Wen Wei Ho, and Soonwon Choi, "Measuring Arbitrary Physical Properties in Analog Quantum Simulation," Physical Review X **13**, 011049 (2023).
[51] Max McGinley and Michele Fava, "Shadow tomography from emergent state designs in analog quantum simulators," (2022), 10.48550/arXiv.2212.02543.
[52] Simon Becker, Nilanjana Datta, Ludovico Lami, and Cambyse Rouze, "Classical shadow tomography for continuous variables quantum systems," (2022), 10.48550/arXiv.2211.07578.
[53] A. Yu. Kitaev, "Fault-tolerant quantum computation by anyons," Annals of Physics **303**, 2–30 (2003).

[54] Jeongwan Haah, "Local stabilizer codes in three dimensions without string logical operators," Physical Review A **83**, 042330 (2011).
[55] Rahul M. Nandkishore and Michael Hermele, "Fractons," Annual Review of Condensed Matter Physics **10**, 295–313 (2019).
[56] Michael Pretko, Xie Chen, and Yizhi You, "Fracton phases of matter," International Journal of Modern Physics A **35**, 2030003 (2020).
[57] Arpit Dua, Isaac H. Kim, Meng Cheng, and Dominic J. Williamson, "Sorting topological stabilizer models in three dimensions," Physical Review B **100**, 155137 (2019).
[58] Arpit Dua, Aleksander Kubica, Liang Jiang, Steven T. Flammia, and Michael J. Gullans, "Clifford-deformed Surface Codes," (2022), 10.48550/arXiv.2201.07802.
[59] John Preskill, "Quantum Computing in the NISQ era and beyond," Quantum **2**, 79 (2018).
[60] Dax Enshan Koh and Sabee Grewal, "Classical Shadows With Noise," Quantum **6**, 776 (2022).
[61] Sivaprasad Omanakuttan, Karthik Chinni, Philip Daniel Blocher, and Pablo M. Poggi, "Scrambling and quantum chaos indicators from long-time properties of operator distributions," (2022), 10.48550/arXiv.2211.15872.
[62] Hrant Gharibyan, Masanori Hanada, Stephen H. Shenker, and Masaki Tezuka, "Onset of random matrix behavior in scrambling systems," Journal of High Energy Physics **2018**, 124 (2018).
[63] Nima Lashkari, Douglas Stanford, Matthew Hastings, Tobias Osborne, and Patrick Hayden, "Towards the fast scrambling conjecture," Journal of High Energy Physics **2013**, 22 (2013).
[64] Tianci Zhou and Xiao Chen, "Operator dynamics in a Brownian quantum circuit," Phys. Rev. E **99**, 052212 (2019).
[65] Lorenzo Piroli, Christoph Sunderhauf, and Xiao-Liang Qi, "A Random Unitary Circuit Model for Black Hole Evaporation," Journal of High Energy Physics **2020**, 63 (2020).